Chemical Engineering Journal 161 (2010) 196–203

Contents lists available at ScienceDirect

Chemical Engineering Journal

journal homepage: www.elsevier.com/locate/cej

Direct measurement of recycle ratios in internal recycle laboratory reactors

Roald Brosius, Jack C.Q. Fletcher*

Centre for Catalysis Research, University of Cape Town, Private Bag X3, Rondebosch 7701, Cape Town, South Africa

ARTICLE INFO

Article history:
Received 4 September 2009
Received in revised form 7 April 2010
Accepted 8 April 2010

Keywords:
Berty reactor
Recycle ratio
Residence time distribution
Internal recycle reactor

ABSTRACT

A method involving the internal positioning of probe capillaries to measure the recycle ratio in an internal recycle reactor equipped with a basket containing a powdered catalyst is reported. The variation of recycle ratio with carrier gas composition, pressure, temperature and catalyst mass is presented. Based on the calculated pressure drop and the principles governing flow resistance across the catalyst bed, the observed relationships between recycle ratio and experimental variables are explained.

1. Introduction

Bench-scale reactors are used to study, test and develop catalysts for industrial scale catalyzed reactions such as, for example, the Fischer-Tropsch synthesis. It is desirable to perform such tests under conditions similar to commercial operation, in particular at space velocities approaching industrial values, and in the absence of heat and concentration gradients to ensure that intrinsic reaction rates are measured. One means to this end is to operate a tubular reactor in differential reactor mode, such that the conversions are sufficiently small for the reaction rates to be considered reasonably constant throughout the catalyst bed. The major disadvantage of this approach is the requirement for measuring small concentration changes in a concentrated feed. By introducing a recycle to the reactor arrangement, a high mass velocity through the catalyst bed, as encountered in commercial operating conditions, can be maintained independent of the fresh feed rate and although differential per-pass conversion is maintained, an overall large concentration change is easily and accurately measured across the experimental system [1].

Moreover, at high recycle ratios all gradients, e.g. concentration and temperature, are minimized if not eliminated. Any remaining gradients are small and calculable in reactors where the internal recycle flow can be measured [2]. It has been shown that at the two extremes of zero and infinitely large recycle, a recycle reactor behaves as a plug flow reactor (PFR) and a well mixed reactor (CSTR), respectively [3].

In laboratory stirred reactors, gas flow through the catalyst bed is brought about by an impeller or by a jet. In the former case, the impeller, whether this is the catalyst basket itself as in the Carberry reactor [4], or a separate impeller as in the Berty reactor [5], provides mechanical mixing. In the jet loop reactor, gas flow is achieved through the venturi effect of the high feed gas velocity entering the reactor through the jet [6], such that under appropriate conditions a jet loop reactor too is an excellent recycle reactor [7].

The well-defined flow path of a recycle reactor lends itself to an easy assessment of the recycle flow, whereas with a CSTR, the mixing may be perfect yet the contact between the catalyst and gas may still be poor or uncertain. Indirectly, the recycle ratio can be obtained from the pressure drop over the catalyst bed or from the adiabatic temperature increase of the reacting gas passing through the catalyst coupled with knowledge of the feed and product stream compositions [5]. Both methods require either tedious calibrations or heat balance calculations, respectively. Good mixing associated with contact between gas and catalyst can also be demonstrated from the absence of external mass transfer limitations in thorough reaction studies, without measuring a recycle ratio [8]. Alternatively, the recycle ratio may be estimated as a model parameter in axial dispersion models [9–11].

Previous attempts at the determination of recycle ratios calculated from the adiabatic temperature rise did not show a clear correlation with impeller speed, suggesting that mixing implied by these recycle ratios is not wholly associated with recycle flow through the catalyst bed but may substantially reflect artifacts associated with gas phase mixing unrelated to recycle flow [12].

This paper presents the results of a study of the residence time distribution (RTD) in a Berty-type internal recycle reactor and addresses the concern that, even though the effluent gas may be well-mixed, contact between gas and catalyst may still be uncer-

---

* Corresponding author. Tel.: +27 21 650 4433; fax: +27 21 650 4051.
E-mail address: jack.fletcher@uct.ac.za (J.C.Q. Fletcher).

1385-8947/$ – see front matter © 2010 Elsevier B.V. All rights reserved.
doi:10.1016/j.cej.2010.04.014

Nomenclature

V	volume
R_r	recycle ratio
q	volumetric flow rate
θ	mean residence time
H	enthalpy
u	linear gas speed
$\dot{m}$	mass flow rate
$\dot{Q}$	heat transfer rate
$\dot{W}_s$	shaft work rate
Q	heat transfer per unit mass
W_s	shaft work per unit mass
C_P	constant pressure heat capacity
C_V	constant volume heat capacity
T	temperature
M	molecular mass
$\vec{u}$	absolute linear gas velocity before impeller
$\vec{w}$	gas velocity relative to impeller blade
$\vec{v}$	impeller blade velocity
u_v	component of absolute velocity in tangential direction
u_a	component of absolute velocity in axial direction
$\dot{P}$	shaft power
τ	shaft torque
ω	angular velocity of impeller
R	gas constant
ρ	density
μ	viscosity
d_p	particle diameter
ε	void fraction
L	bed length
Re	Reynolds number
κ	permeability coefficient
A	catalyst basket surface area
k	ratio of heat capacities, C_P/C_V

tain. Recycle ratios were found directly from response curves of pulse injections to the reactor system using the pulse to pulse period of initial recycle pulses. The variation of recycle ratios with pressure, temperature, gas composition and catalyst bed resistance (catalyst mass) was determined in relation to the impeller rotational speed. Moreover, recycle ratios are also obtained at reaction conditions for high temperature Fischer-Tropsch synthesis in an internal recycle reactor.

2. Experimental

The CSTR behaviour of the reactor was studied employing a precipitated iron catalyst under high temperature Fischer-Tropsch reaction conditions by varying the impeller speed. Fig. 1 shows a scaled schematic drawing of the reactor indicating the position of the capillaries. The reactor has a volume of 840 ml determined gravimetrically from water filling. The feed flow rate was kept constant at 1500 standard cubic centimetres per minute (sccm), equivalent to a space velocity of 300 sccm/g in Fischer-Tropsch tests. Methane tracer pulses were injected through a six-way valve capable of withstanding high temperature and pressure in close proximity to the stirred internal recycle reactor (STIRR). A flexible capillary (15 m VARIAN FactorFour 0.25 mm ID) was used to sample the response of tracer gas from the reactor. Multiple capillaries were connected in series when the reactor was operated at elevated pressures (10–30 bar) in order to limit sample flow to the flame ionization detector (FID) of a VARIAN 3900 gas chromatograph, the latter controlled by a computer directing the methane injection and tracer data collection. In this manner injection and tracer data collection were synchronized and time lags between pulse injection and tracer detection were repeatable.

The catalyst basket (7 cm diameter) comprises two circular 3 mm aperture grids each holding a 15 μm sintered stainless steel felt (of 15 μm aperture) in place. The iron catalyst (5 g), placed between the upper and lower sieve/felt closures, has a mean particle diameter of 35 μm after sieving so as to remove the fraction smaller than 25 μm. The catalyst fills the apertures of the sieve, uniformly covering the basket floor area to a depth of 2 mm.

The input methane tracer pulse width was measured to be 3 s by sampling from a tee-piece at the inlet tube – virtually no tailing of the input peak was evident. Thus the flow through the capillary is considered plug flow and leads only to a time lag in the response.

Fig. 2a presents the FID signal of the reactor system's response to a methane pulse, with the initial 3 min of the trace expanded in Fig. 2b. When a mixed reactor such as the STIRR is represented by a plug flow reactor with recycle R_r, the time needed for a single transit of the methane pulse is given by Eq. (1)

$$\frac{V}{(1+R_r)q} = \frac{\theta}{(1+R_r)} \tag{1}$$

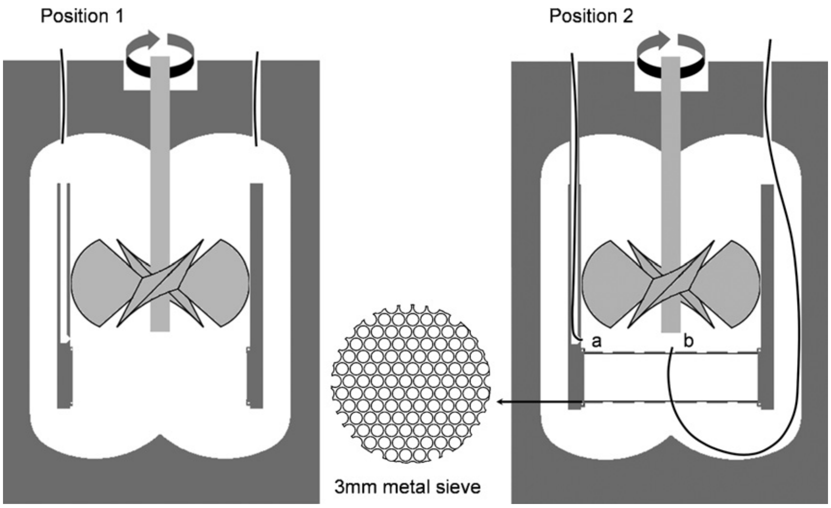

Fig. 1. Scaled schematic drawing of STIRR showing capillary arrangements (positions 1 and 2).

The recycle ratio R_r can then be calculated from the response pulse to pulse period using Eq. (2)

$$R_r = \frac{\theta}{\Delta t} - 1 \tag{2}$$

Fig. 2a indicates that the STIRR closely approximates a CSTR.

3. Results and discussion

3.1. Capillary positioning to measure the recycle ratio

The recycle ratio was first measured in an empty reactor – without felts or sieves but with the internal cylinder in place – with both the inlet and the outlet capillaries positioned in the lid of the reactor within the gas inlet and outlet tubing, an arrangement referred to as position 1 in Fig. 1. In Fig. 3, a comparison of the recycle ratios measured at steady state in flowing hydrogen with those in flowing nitrogen for an empty STIRR shows that higher recycle ratios are obtained with nitrogen. The data also display the range within which the recycle ratio can be measured with reasonable error. Beyond this range, at higher impeller speeds, the tracer recycle pulses are no longer clearly distinguishable in the product tracer signal. When one sintered metal felt is installed in the path of the gas stream passing through the catalyst basket, the resulting substantial flow resistance is evidenced by the dramatically lower recycle ratios presented in Fig. 3. With two sintered metal felts serving as base and top of the catalyst basket, recycle gas flow is still further reduced. With hydrogen feed gas, recycle ratios could not be measured when one or more sintered metal felts are placed in the catalyst basket. Dissipation of the tracer recycle pulses is presumably due to a larger diffusion of methane in hydrogen as compared to the case in nitrogen.

In order to overcome this experimental limitation, the outlet capillary was moved around in the reactor to find a better position for detecting the initial tracer recycle peaks. A minimum of two tracer recycle peaks need to be detected in order to measure the time interval between tracer recycle peaks which is needed to calculate the recycle ratio. With both the inlet and the outlet capillary at the top of the reactor, the first recycle peak has made one full circuit of the recycle flow path before it is detected. By positioning the inlet capillary to just above the upper felt of the catalyst basket (via a tube inserted through the thermo-well in the cylindrical wall of the internal catalyst basket) and with the outlet capillary positioned above the catalyst bed (by pushing it from below through the sintered metal felts of the catalyst basket into the centre of the reactor underneath the impeller), the first tracer pulse is detected immediately upon tracer entrance into the reactor, and the time required to establish the recycle period is roughly halved, thereby considerably reducing the tracer pulse dissipation between subsequent recycle circuits. The arrangement of inlet and outlet capillaries in this close proximity is illustrated in Fig. 1 by (a) and (b) respectively, and is referred to as position 2. The advantage of such a close arrangement is illustrated in Fig. 3. For instance, the measurable range is much larger when inlet and outlet are in close proximity, in position 2 with one felt installed compared to the case when inlet and outlet are at the top of the reactor, position 1. More importantly, with hydrogen, tracer pulses are only observed with the inlet and outlet capillary in the close arrangement of position 2.

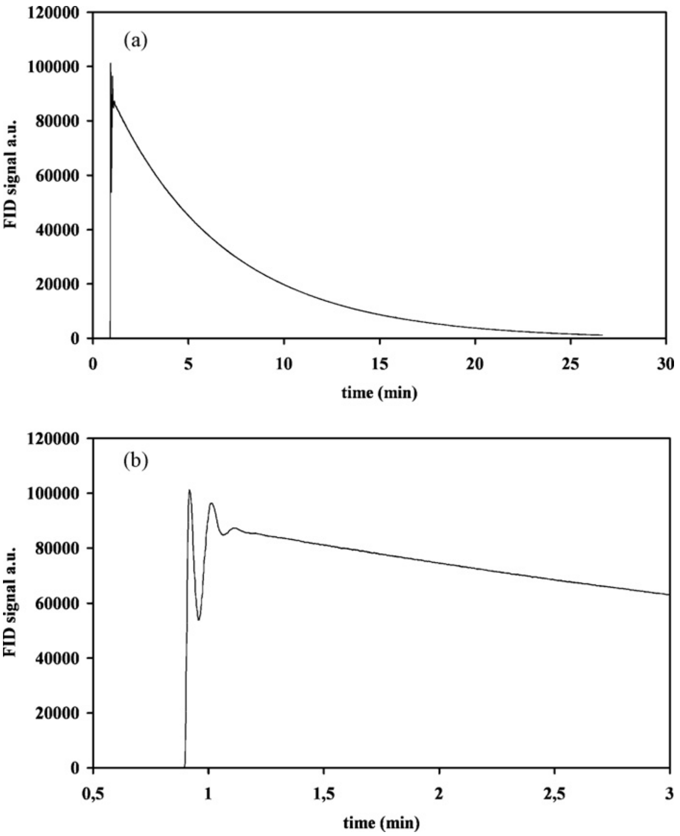

Fig. 2. (a) FID response signal to methane pulse to STIRR, RT, θ = 6.16 min, Δt = 0.094 min, R = 65, impeller: 4.5 Hz = 160 rpm, no felts in catalyst basket, both inlet and outlet in the lid of the reactor. (b) Recycle pulses in first 2.75 min of FID signal response to methane pulse.

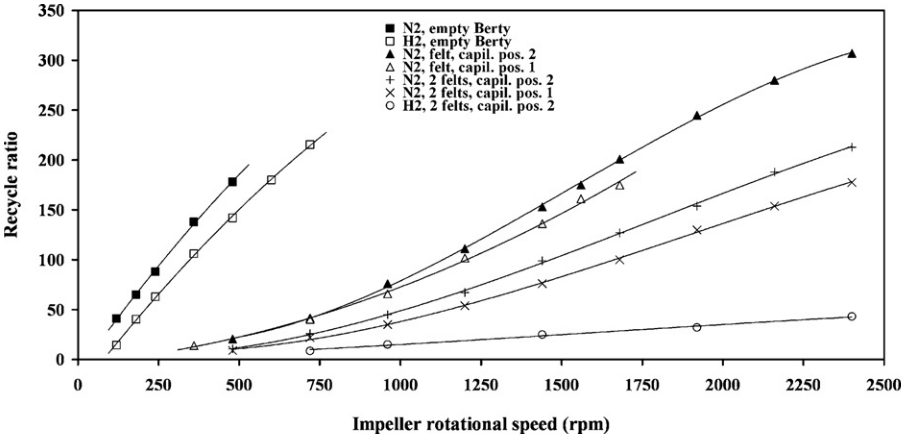

Fig. 3. Recycle ratio versus impeller speed for hydrogen and nitrogen as carrier gas in an empty reactor or with sintered metal felts in the catalyst basket and with capillary arranged in the reactor lid (position 1) or in close proximity above the catalyst basket (position 2), *P*; 10 bar, *T*; 25 °C.

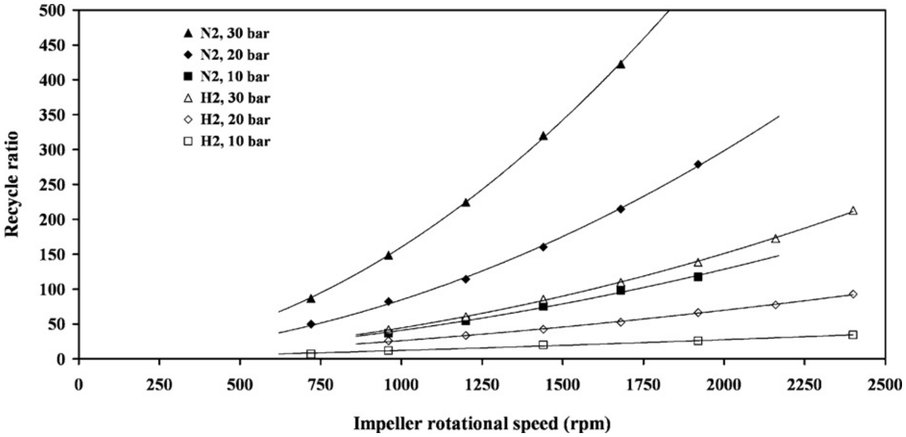

Fig. 4. Recycle ratio versus impeller speed for hydrogen and nitrogen at different pressures; inlet and outlet in close arrangement, 5 g catalyst between 2 sintered metal felts.

It was observed however, that recycle ratios are systematically higher when measured with capillaries in position 2 than when obtained from capillaries in position 1. This is an artefact of the experimental method and may be explained by the fact that the inlet and outlet capillaries in position 2 are still separated by 3 cm – the inlet capillary being at the periphery of the internal recycle loop and the outlet capillary being in the centre such that the first recycle period is systematically shorter than the second recycle period by about 25%, resulting in an equally large overestimation of the recycle ratio. The separation of the capillaries by 3 cm avoids that the tail of the highly concentrated initial tracer input pulse obscures the first tracer recycle pulse, a problem that occurs especially with hydrogen because of the faster diffusion of methane in hydrogen. Under most conditions, a third tracer recycle pulse cannot be distinguished in the outlet tracer signal, leaving only the first recycle period from which to determine the recycle ratio. With nitrogen carrier gas, the problem of an excessively large input pulse is less pronounced and the outlet capillary could be moved closer to the inlet capillary. Under conditions of the inlet and outlet capillaries being almost co-incident, the first and second recycle periods are the same and equal to the recycle period measured with capillaries in position 1.

The recycle ratio is thus essentially the same when measured in the internal recycle loop (capillary position 2), or outside of the internal recycle loop at the extremities of the inlet and outlet of the reactor (capillary position 1). This demonstrates emphatically that the impeller not only mixes the gas in the STIRR but that the impeller effectively drives the gas through the catalyst basket despite the high flow resistance offered by the packed catalyst bed and, consequently, that the recycle ratio may confidently be extracted from residence time distribution data.

3.2. *Effect of pressure on the recycle ratio*

The recycle ratio was determined at different pressures and temperatures with 5 g of a powdered Fischer-Tropsch catalyst in the basket comprising base and top mesh/felts to contain the catalyst, and with the inlet and outlet capillaries arranged in position 2. Fig. 4 presents the influence of impeller speed on recycle ratio at increasing pressures for both hydrogen and nitrogen feed gas. The recycle ratio increases with pressure and molar mass suggesting that the recycle ratio depends on the density of the gas. However, the recycle ratio does not vary linearly with pressure – from 10 to 20 bar the recycle ratio roughly doubles (from 54 to 114) but from 10 to 30 bar the recycle ratio increases approximately fourfold (from 54 to 224).

In order to relate the recycle ratio to any or multiple intensive properties of the gas, such as pressure, temperature, density, molar mass and viscosity, an energy balance over an open system is applied. The control volume is chosen so that it encompasses the impeller but not the catalyst basket. In this way it is possible to determine the energy transferred to the gas as work done on the gas by the impeller and which, in turn, generates an increased pressure above the catalyst basket. A pressure drop over the catalyst basket results from the resistance to flow around the internal recycle loop offered by the sintered metal felts and the catalyst.

The first law of thermodynamics for a steady-state flow process with one entrance and exit, and with shaft work (impeller work) being the only form of work done on the system but neglecting potential energy terms, reads

$$\Delta H + \frac{\Delta u^2}{2} = Q + W_s \tag{3}$$

All terms represent energy per unit mass of fluid [13]. Assuming that no heat is removed from or added into the control volume ($Q = 0$), work is done on the system to increase the enthalpy and to increase the kinetic energy of the fluid. It is useful to define the stagnation (total) enthalpy as the sum of the enthalpy of the moving fluid and its kinetic energy.

$$H_t \equiv H + \frac{u^2}{2} \tag{4}$$

The stagnation (total) temperature of a flowing fluid is defined as the temperature that would result if the fluid were brought to rest adiabatically and reversibly. This temperature is calculated using the constant-pressure molar heat capacity: C_P from:

$$\Delta H = C_P \Delta T \tag{5}$$

Combining Eqs. (4) and (5) leads to

$$T_{t_1} = T_1 + \frac{u^2 M}{2C_P} \quad \text{and} \quad T_{t_2} = T_{t_1} + W_s \frac{M}{C_P} \tag{6}$$

Since $u^2M/2C_P$ is much smaller than T_1 (see Table 1), T_1 is approximately equal to T_{t_1}. Under the simplifying assumption that the work done on the gas is mechanically reversible and occurs adiabatically, the enthalpy change of the gas flow can be expressed as:

$$dH = C_P dT = V dP \tag{7}$$

From Eq. (7) and the ideal gas law, the adiabatic equation can be derived for calculating the final pressure, P_2, from the initial pres-

Table 1
Pressure drop calculation for nitrogen and hydrogen.

$P = 100 \times 10^6$ Pa	$d_{\text{blade}} = 700$ cm	$\nu = 1920$ Hz
$T_1 = 298.15$ K	$d_{\text{shaft}} = 100$ cm	$R = 8.31 \times 10^3$ J/kmol K
$q_{\text{in}} = 1500$ ml/min (STP)	$r_{\text{ave}} = 200$ cm	$k = C_P/C_V = 140$
$q_{\text{in}} = 250 \times 10^{-6}$ (m³/s) at 10 bar	$A = 385 \times 10^{-3}$ m²	
	N_2	H_2
M (kg/kmol)	28	2
C_P (kJ/kmol K)	29,125	28,824
ρ (kg/m³)	11.3	0.81
R_r	117	26
u_1 (m/s)	7.63×10^{-2}	1.66×10^{-2}
v (m/s)	4.02	4.02
u_{v_2} (m/s)	3.94	4.00
u_{a_2} (m/s)	4.17	4.05
W_s (J/kg)	23.95	24.19
ΔP (Pa)	277	20

sure, P_1, and the ratio of the stagnation temperatures, T_{t_2}/T_{t_1}.

$$\frac{P_2}{P_1} = \left(\frac{T_{t_2}}{T_{t_1}}\right)^{k/k-1} \quad \text{with} \quad k = \frac{C_P}{C_V} \tag{8}$$

The work done on the gas can be calculated from a velocity diagram as the one shown in Fig. 5. Gas molecules approaching with an absolute velocity $\vec{u}_1$ collide with the impeller, having a blade velocity $\vec{v}$, and leave with an absolute velocity $\vec{u}_2$. The relationship among the absolute velocity $\vec{u}$, relative velocity $\vec{w}$, and blade velocity $\vec{v}$ is given by the following vector equation:

$$\vec{u} = \vec{v} + \vec{w} \tag{9}$$

We assume that the magnitude of the relative velocities to the blade, $\vec{w}_1$ and $\vec{w}_2$, is conserved but that the direction is mirrored on the normal to the blade as seems plausible when observed from the moving reference frame of the blade. Work is done on the gas in the tangential direction, W_{tan}, and in the axial direction, W_{axial}, with the former raising the enthalpy of the gas whereas the latter increases the gas kinetic energy. Combining W_{tan} and W_{axial} gives W_s. In an ideal compressor stage consisting of a rotor and a stator, all work done on the gas is done by the rotor, the stator converting the kinetic energy into enthalpy thereby raising the pressure.

The rate of energy transfer for a rotor in the tangential direction is the product of the torque and the angular velocity [14]. Thus, with u_{v_2} and u_{v_1} being the components of the absolute velocities $\vec{u}_1$ and $\vec{u}_2$ in the tangential direction (the direction of the whirl v), respectively

$$\dot{P} = \omega\tau_{shaft} = \dot{m}(\omega r u_{v_2} - \omega r u_{v_1}) \tag{10}$$

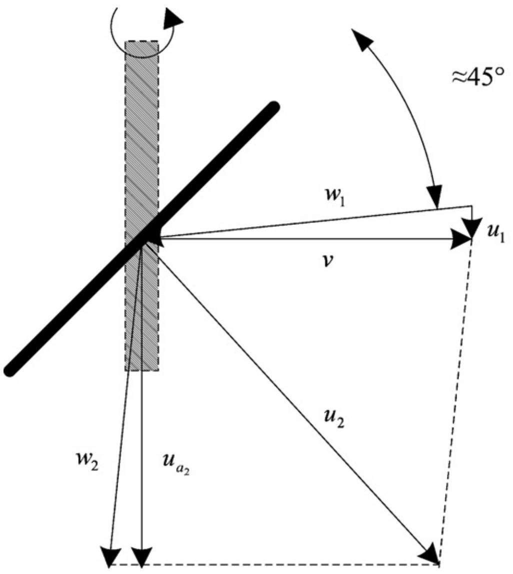

Fig. 5. Velocity diagram of the impeller.

Since the blade velocity v is $v = \omega r_{ave}$, (and $u_{v_1} = 0$) the rate of energy transfer becomes:

$$\dot{P} = \omega\tau_{shaft} = \dot{m}_2 v u_{v_2} \tag{11}$$

or, per unit mass,

$$W_{\text{tan}} = v u_{v_2} \tag{12}$$

The work done on the gas, per unit mass, in the axial direction is given by

$$W_{axial} = \frac{u_{a_2}^2}{2} - \frac{u_1^2}{2} \tag{13}$$

where u_{a_2} is the component of the absolute velocity $\vec{u}_2$ in the axial direction. Thus the total work done on the gas in the STIRR can be calculated from the impeller speed and the gas velocity. Combining Eqs. (6) and (8), and with $T_{t_1} \approx T_1$, an expression for the pressure rise is obtained.

$$\Delta P = P_1\left(\left(\frac{T_{t_2}}{T_{t_1}}\right)^{k/k-1} - 1\right) = P_1\left(\left(1 + \frac{W_s M}{C_P T_1}\right)^{k/k-1} - 1\right) \tag{14}$$

The function $f(x) = (1 + cx)^n$, with $x = M$, $c = W_s/C_P T_1$ and $n = k/k-1$, may be defined by a Maclaurin series. Since c is much smaller than 1 (see Table 1), all terms from c^2 upwards may be neglected and the power series reduces to

$$\sum_{n=0}^{\infty} \frac{f^{(n)}}{n!}(x)^n = \frac{(1+c0)^n}{0!}x^0 + \frac{nc(1+c0)^{n-1}}{1!}x^1 + \frac{n(n-1)c^2(1+c0)^{n-2}}{2!}x^2 + \cdots = 1 + ncx$$

Hence, Eq. (14) reduces to

$$\Delta P = P_1 M \left(\frac{k}{k-1}\frac{W_s}{C_P T_1}\right) \tag{15}$$

Using the ideal gas law $PV = nRT$ and $m = nM$, $PM = \rho RT$, Eq. (15) may be further simplified to

$$\Delta P = \frac{k}{k-1}\frac{\rho R}{C_P} W_s \tag{16}$$

The rotational speeds at which the STIRR impeller is operated are roughly two orders of magnitude higher than the gas velocity. As a result, the relative velocity at which the gas approaches the impeller is at nearly right angles to the axial direction. Since the impeller blades whirl at 45° to the axial direction, gas molecules collide with the impeller and leave with an absolute velocity of almost 45° to the vertical axis. Therefore, the tangential component of the gas velocity u_{v_2} is almost exactly the same as the axial component u_{a_2} and approximately equal to the impeller speed v. Consequently, the energy transferred to the gas as work done on the gas is consumed to increase the enthalpy of the gas (which raises the static pressure) and the kinetic energy of the gas (which can be understood as dynamic pressure) in almost equal parts. More importantly however, because the impeller speed is much larger than the gas velocity, the work done on the gas, per unit mass, is dominated by the impeller speed. Table 1 presents an example of the calculation of the pressure drop for N_2 and H_2. As expected, the

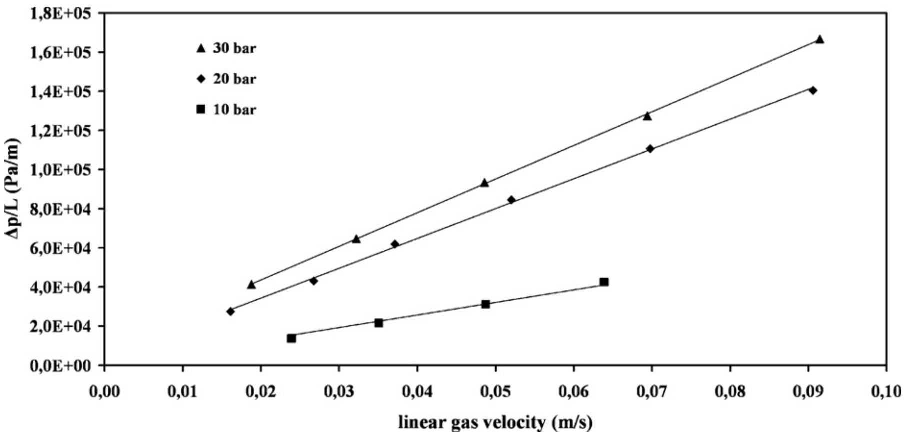

Fig. 6. Pressure drop over bed length versus linear gas velocity at reactor pressure (10, 20 and 30 bar), 25 °C and with 5 g of catalyst.

Table 2
Variation of the viscosity (μ) of hydrogen and nitrogen with temperature [15].

Temperature (°C)	25	100	200	300
$\mu(H_2)$ (kg/sm)	7.2×10^{-6}	8.4×10^{-6}	9.8×10^{-6}	11.1×10^{-6}
$\mu(N_2)$ (kg/sm)	17.2×10^{-6}	20.4×10^{-6}	24.1×10^{-6}	27.5×10^{-6}

pressure drop generated by the impeller is much higher for N_2 on account of its larger molecular mass.

Under steady state operation, the pressure head generated by the impeller is equal to the velocity head that produces flow through the catalyst basket. Combining a calculation of the driving force with an assessment of the resistance to flow ultimately results in a relation between the impeller speed and the superficial linear gas velocity.

Pressure drop arising from resistance to flow through a packed bed can be estimated by the Ergun equation

$$\frac{\Delta P}{L} = 150\frac{(1-\varepsilon)^2}{\varepsilon^3}\frac{\mu u}{d_p^2} + 1.75\frac{(1-\varepsilon)}{\varepsilon^3}\frac{\rho u^2}{d_p} \quad (17)$$

However, in our case, the sintered metal felt offers substantially more resistance than the catalyst (see Section 3.4) and cannot be compared to a packed bed. Also, the Ergun equation is strictly applicable only to flow through packed beds in the porosity range of approximately 0.35–0.5, whereas the sintered metal felt in our experiments has a void fraction of ±0.75. The form of the Ergun equation shows that viscous resistance and inertial resistance are superimposed. Fig. 6 displays the pressure drop calculated with Eq. (16), per unit length, as a function of the linear gas velocity obtained from the measured recycle ratio. The good linear correlation between the pressure drop and the linear gas velocity demonstrates that viscous resistance dominates over inertial resistance. This is further substantiated by the fact that, for the experiments conducted, the Reynolds number $Re = \rho d_p u/\mu(1-\varepsilon)$ is never greater than 12, well within the Darcy regime of laminar flow. The slope of the linear regression varies with total pressure because the pressure drop is a function of pressure; Eq. (15). However, the slope of the 30 bar $\Delta P/L$ line is lower than expected and the recycle ratio increases more strongly than expected from 20 to 30 bar as noted above.

The basic law governing permeability calculations for laminar, viscous flow is that of Darcy, which states that the linear gas velocity is directly proportional to the pressure gradient causing flow. With an impeller rather than a compressor stage, Δp is small compared to p and the following holds:

$$u = -\frac{\kappa}{\mu}\frac{\partial p}{\partial x} = \frac{\kappa}{\mu}\frac{\Delta p}{L} \quad (18)$$

where κ is the permeability coefficient for viscous flow.

Table 2 lists gas viscosities at different temperatures for H_2 and N_2. Gas viscosity is independent of pressure and the viscosity of N_2 is about 2.5 times that of H_2. Combining Eqs. (18) and (16) gives a correlation between the linear gas velocity and the gas density, viscosity and work done

$$u = \frac{\rho}{\mu}\frac{\kappa}{L}\frac{k}{k-1}\frac{R}{C_P}W_s \quad (19)$$

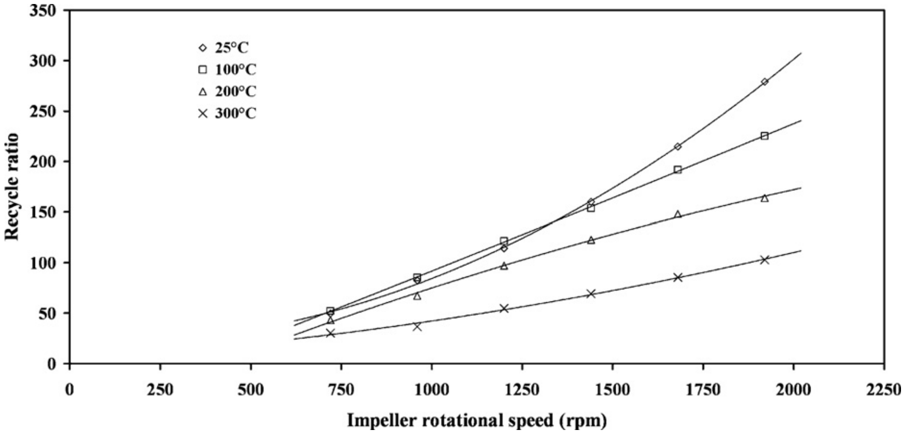

Fig. 7. Recycle ratio versus impeller speed at different temperatures; nitrogen carrier gas, $P = 20$ bar, 5 g of catalyst between 2 sintered metal felts, inlet and outlet capillary in close arrangement.

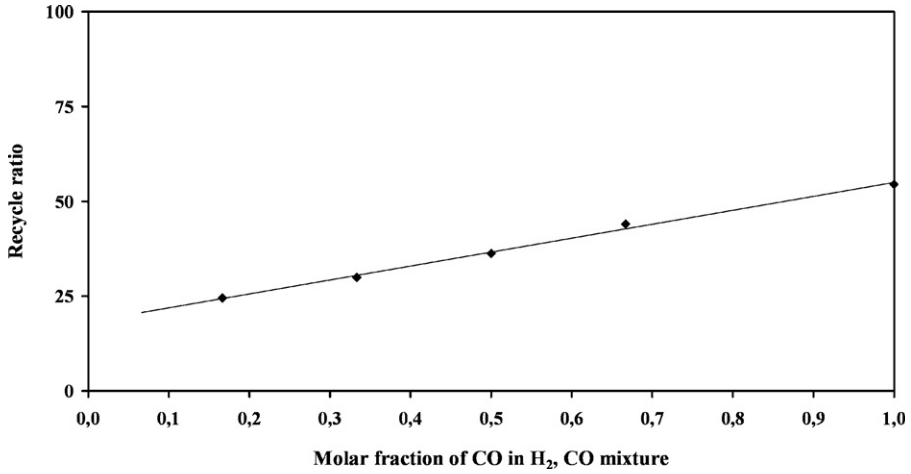

Fig. 8. Recycle ratio versus molar composition of CO in H_2/CO mixture, impeller speed: 720 rpm, RT, no catalyst, 2 sintered metal felts, inlet and outlet capillary in close arrangement.

This correlation rationalizes the observations from Fig. 4, namely that the recycle ratio ($R_r = uA/q_{in}$) increases with pressure and that the recycle ratio with N_2 is larger than with H_2 – because the ratio of density to viscosity is larger for N_2 than for H_2. The correlation also explains the quadratic dependency on impeller speed v, from the calculation of W_s, as is clearly shown in Fig. 4.

3.3. Effect of temperature on the recycle ratio

Fig. 7 shows a plot of recycle ratio as a function of impeller speed at 20 bar in nitrogen feed gas at different temperatures, from which it can be seen that the recycle ratio decreases with increasing temperature. This is consistent with Eq. (19), where decreased gas density and increased gas viscosity contribute to lowering the linear gas velocity upon increasing temperature.

3.4. Effect of catalyst mass and of gas composition on the recycle ratio

By doubling the catalyst mass, the recycle ratio is reduced only by 10%, indicating that the pressure drop across the catalyst basket is largely due to the sintered metal felts and that the catalyst, even though it is a very fine powder, contributes only marginally.

In view of this reactor finding its purpose in the study of catalysts for the high temperature Fischer-Tropsch synthesis, the recycle ratio was measured for various compositions of a CO and H_2 syngas mixture. The results are presented in Fig. 8. Recycle ratios decrease with increasing molar fraction of hydrogen in the mixture. At a ratio of H_2/CO of 2, typical of Fischer-Tropsch synthesis, the recycle ratio is about half of that with pure CO. Conversion of syngas to hydrocarbons and water will increase the density as the partial pressure of hydrogen is lowered and therefore the recycle ratio is expected to increase from its minimum before conversion of fresh syngas.

3.5. Effect of residence time on the recycle ratio

The effect of residence time on the recycle ratio, which can be measured by varying the feed gas mass flow rate at set pressures, was not independently determined. However, from the above discussion it is clear that the work done by the feed gas on the control volume is negligible compared to the work done by the impeller. It may therefore be safely assumed that there is no significant effect of the feed gas mass flow rate on the recycle ratio. By contrast, the recycle ratio measured in the jet loop reactor is inversely proportional to the residence time [7]. In such a system the feed gas does expansion work at the inlet jet and a higher mass flow rate requires a larger pressure difference over the jet resulting in more work being done. The feed gas is accelerated through the jet and propelled along the internal recycle loop giving rise to higher recycle ratios at short residence times.

4. Conclusions

By internally positioning tracer inlet and outlet capillaries in close proximity of each other in the internal recycle flow path above the catalyst basket, the recycle ratio could be measured in hydrogen carrier despite the rapid diffusion of the methane tracer pulse in hydrogen. It was demonstrated, emphatically, that the impeller not only mixes the gas in the STIRR, but that the impeller effectively drives the gas through the catalyst basket despite the flow resistance offered by the packed catalyst bed and, consequently, that the recycle ratio may confidently be extracted from pulse response traces. From thermodynamic and physical principles the work done on the gas can be calculated and correlated to the linear gas velocity such that the linear gas velocity and, consequently, the recycle ratio was found to be directly proportional to gas density and inversely proportional to gas viscosity. It follows thus, that the recycle ratio increases with pressure and decreases with temperature. Even at conditions appropriate to the high temperature Fischer-Tropsch synthesis (20 bar, 330 °C, and $H_2/CO \approx 2$) with a powdered catalyst, a recycle ratio in excess of 25, the generally accepted minimum value required value to satisfy the limiting condition for negligible concentration and temperature gradients, can easily be achieved at impeller rotational speeds greater than 720 rpm.

Acknowledgements

The authors gratefully acknowledge the financial and the technical support of Sasol Technology (Pty) Limited in this study as well as the financial support of the Technology For Human Resource Industry Programme (THRIP, 70265 and 70093). We thank Ms. Hema Vallabh for diligently assisting in the laboratory.

References

[1] J.M. Berty, Catal. Rev. Sci. Eng. 20 (1) (1979) 75.
[2] J.M. Berty, Plant/Operations Progress 3 (3) (1984) 163.
[3] B.M. Gillespie, J.J. Carberry, Ind. Eng. Chem. Fundam. 5 (1966) 164.
[4] J.J. Carberry, Ind. Eng. Chem. 56 (1964) 39.
[5] J.M. Berty, Chem. Eng. Prog. 70 (5) (1974) 78.
[6] G. Shermuly, G. Luft, Chem. Eng. Tech. 49 (1977) 907.

[7] K.P. Möller, J.C.Q. Fletcher, C.T. O'Connor, R.J. Becker, Chem. Eng. Commun. 137 (1995) 111.

[8] H. Hannoun, J.R. Regalbuto, Ind. Eng. Chem. Res. 31 (1992) 1288.

[9] C.H. Kersting, J. Prüss, H.-J. Warnecke, Chem. Eng. Sci. 50 (1995) 299.

[10] T. Zhang, T. Wang, J. Wang, Chem. Eng. Sci. 44 (2005) 1221.

[11] P.A. Melo, J.C. Pinto, E.C. Biscaia Jr., Chem. Eng. Sci. 56 (2001) 2703.

[12] Prinsloo, F., Koning, B., Development and Testing of a Stirred-from-Top Berty Micro Reactor, Internal report, Chemicals from Synthesis Gas Group, Research and Development, Sasol (2005).

[13] J.M. Smith, H.C. Van Ness, M.M. Abbott, Introduction to Chemical Engineering Thermodynamics, 7th ed., McGraw-Hill, 2005.

[14] W.H. Bathie, Fundamentals of Gas Turbines, John Wiley & Sons, 1984.

[15] R.H. Perry, C.H. Chilton, Chemical Engineers Handbook, 5th ed., McGraw-Hill, 1973.